Available online at www.sciencedirect.com

ScienceDirect

Procedia Structural Integrity 26 (2020) 321–329

Structural Integrity Procedia

www.elsevier.com/locate/procedia

The 1st Mediterranean Conference on Fracture and Structural Integrity, MedFract1

Simulating the dependence of the filler wire feeding on the wire size in the hybrid metal extrusion & bonding (HYB) process

Francesco Leoni[a]*, Øystein Grong[a,b], Paolo Ferro[c], Filippo Berto[a]

[a]*Department of Mechanical and Industrial Engineering, Norwegian University of Science and Technology, Richard Birkelands vei 2b, 7491 Trondheim, Norway*

[b]*HyBond AS, NAPIC, Richard Birkelands vei 2b, 7491 Trondheim Norway*

[c]*Department of Management and Engineering, University of Padova, Stradella S. Nicola, 2 I-36100 Vicenza, Italy*

Abstract

HYB is a new solid-state joining method for metals and alloys that utilizes continuous extrusion as a technique to enable aluminium filler metal (FM) additions. In the present work, a finite element (FE) model for the filler wire feeding inside the HYB PinPoint extruder has been developed and implemented within the commercial software package DEFORM 3D™. Adaptive remeshing is used to handle the high mesh distortions occurring during simulation. Moreover, modelling of the FM flow stress as a function of strain, strain rate and temperature is done by employing a modified version of the Johnson-Cook constitutive equation and experimental tensile test data for the AA6082 filler wire. In the numerical simulations, the feeding behaviour of filler wires with diameters of 1.2, 1.4 and 1.6 mm, respectively has been explored. The results show that the filler wire feeding is sensitive to variations in the extrusion chamber geometry. For the specific combinations of wire diameters and extrusion chamber geometries examined, the ϕ1.4 mm wire appears to be the best choice when it comes to reducing feeding problems related to buckling & breaking of the filler wire during extrusion & joining.

Keywords: Finite Element Modelling; Continuous Extrusion; Aluminium Filler Wire Feeding; Hybrid Metal Extrusion and Bonding.

* Corresponding author. Tel.: +393473335042
E-mail address: francesco.leoni@ntnu.no

10.1016/j.prostr.2020.06.041

1. Introduction

The term solid-state joining covers a vast number of processes such as cold pressure welding, diffusion welding explosion welding, forge welding, conventional friction welding and friction stir welding, hot pressure welding, roll welding and ultrasonic welding AWS Welding Handbook (2007), ASM Metals Handbook (1993). All these processes enable coalescence at temperatures essentially below the melting point of the base materials to be joined, without the addition of a brazing filler metal Grong (2012). Because there is no melting involved, the metals being joined will largely retain their microstructural integrity without forming a fusion zone and a wide heat-affected zone with degraded properties, which is the main problem with traditional fusion welding Grong (1997). Also in dissimilar metals joining the solid-state methods offer considerable advantages compared to fusion welding due to the reduced risk of excessive intermetallic compound formation and subsequent interfacial cracking - all being the result of large differences in chemical composition, crystal structure, thermal expansion and conductivity between the two components to be joined Mazar et al (2014).

Recently, a new solid-state joining method for metals and alloys has appeared on the horizon, known as the Hybrid Metal Extrusion & Bonding (HYB) process Grong (2012), Sandnes et al. (2018), Berto et al. (2018), Blindheim et al. (2018), Grong et al. (2019), Sandnes et al. (2019), Grong et al. (2019). The HYB method utilizes continuous extrusion as a technique to enable filler metal (FM) additions. Figure 1 highlights the most important HYB PinPoint extruder tool parts as well as the flow behaviour of the FM inside the welding head.

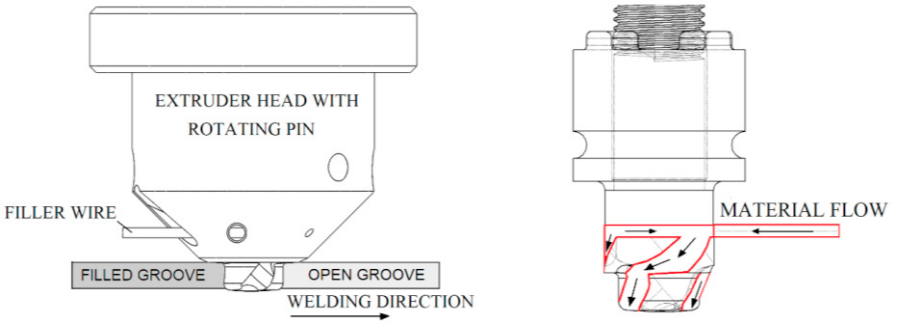

Figure 1: Schematic representations of the main HYB PinPoint extruder tool parts. Included is also a sketch of the flow behaviour of the FM inside the extrusion chamber and through the moving dies in the pin.

In a real butt welding situation, the plates to be joined are separated from each other by a fixed spacing so that an I-groove forms between them. During joining, the extruder head slides along the joint line at a constant travel speed. At the same time the rotating pin with its moving dies is placed in a submerged position below. This allows the extrudate to flow downwards in the axial direction and into the groove under high pressure and mix with the base metal (BM). Metallic bonding between the FM and the BM then occurs by a combination of oxide dispersion and severe plastic deformation Sandnes et al. (2018), Sandnes et al. (2019), Grong et al. (2019). By proper adjustment of the wire feed rate (using the rotational speed of the drive spindle as the main process variable), the entire cross-sectional area of the groove can be filled with solid aluminium in a continuous manner Grong et al. (2019).

It follows from Figure 1 that the PinPoint extruder is the core of the HYB invention. Until now the development has been done using rapid prototyping and laboratory testing, in accordance with well-established design methodology Ulrich and Eppinger (2008). Recently, a FE approach has been developed, focusing on the filler wire feeding, since this is the most delicate and crucial part of the entire HYB process Leoni et al. (2020a). In the present paper, the approach is further explored and pushed to its limits by running full-scale simulations of the wire feeding inside the HYB PinPoint extruder, using the filler wire diameter as the main process variable. The material properties used as inputs to the simulations have been upgraded by considering the true stress-strain behaviour of the FM, based on constitutive modelling and the tensile test results reported previously by Leoni et al. (2020b). In the present paper some new simulation results are presented following this upgrading. At the same time their relevance in the context of the HYB process is discussed and documented by comparison with experimental observations.

2. FE modelling

A full 3D analysis of HYB wire feeding system is performed employing Version 12 of the commercial software package DEFORM 3D™.

2.1. Geometric modelling and simulation conditions

As a starting point the Lagrangian code is used along with an adaptive remeshing technique. This is necessary in order to handle the high mesh distortions which occur during simulation. A fully coupled temperature-displacement analysis is implemented to allow both the temperature and the displacement at each node to be calculated simultaneously at every step increment. Moreover, to provide realistic physical representations of the essential extruder parts involved during the extrusion operation, the CAD files of the HYB PinPoint extruder are imported directly into DEFORM 3D. The different tool parts are shown in Figure 2.

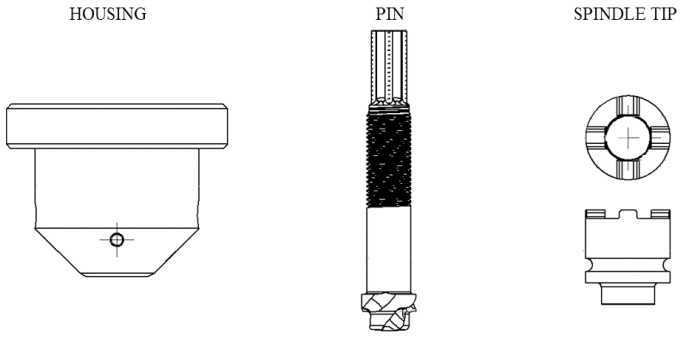

Figure 2: Schematic drawings of the extruder tool parts being imported into Deform 3D™ and employed in the simulations.

The geometry of the extrusion chamber is also an important issue in the HYB case because it is crucial for the filler wire feeding. In the present simulations, the conically-shaped extrusion chamber employed by Støren (1976) is used as a basis for downscaling the geometry so that it fits wire diameters of 1.2, 1.4 and 1.6 mm, respectively. These are the most relevant wire sizes in the HYB case. Figure 3 (a) shows a schematic drawing of the chamber and the critical dimensions that need to be adjusted for each wire diameter, whereas Figure 3 (b) shows a corresponding drawing of a section through the extrusion chamber.

In addition, the drive spindle rotational speed N_s has been adjusted to accommodate the different wire diameters, using the formulae reported by Grong et al. (2019) for the dependence of the deposition rate on the HYB process parameters. Note that the values for N_s used in the present simulations provide the same volume flow of extrudate per unit time through the extruder for all three wires. Hence, the rotational speed is highest for the ϕ1.2 mm wire and lowest for the ϕ1.6 mm wire. Table 1 summarizes the simulation conditions employed in FE analysis.

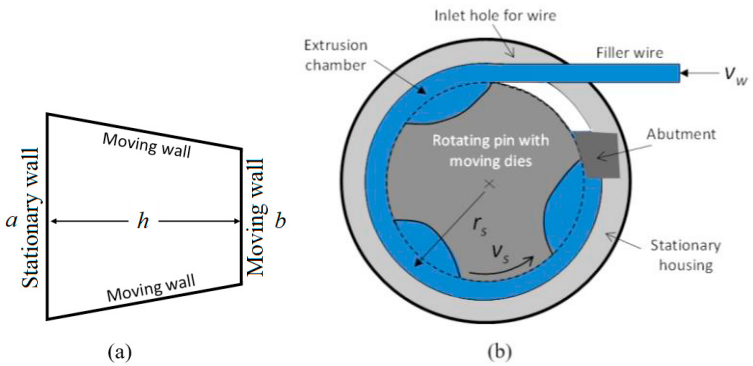

Figure 3: Schematic drawings of (a) the conically-shaped extrusion chamber used in the simulations and (b) a section through the extrusion chamber.

Table 1: Simulation conditions used in the FE analysis.

Physical objects	Parameter	Type or Value
Workpiece (Wire)	Material	AA6082
	Diameters	1.2; 1.4; 1.6 [mm]
	Mesh type	Tetrahedral
	Friction factor*	0.4
	Initial temperature	293 [K]
	Thermal expansion	22 [μm/m K]
	Thermal conductivity	180 [W/m K]
	Heat capacity	889 [J/kg K]
Extruder parts	Material	AISI 316-Rigid
	Friction factor**	0
	Initial temperature	293 [K]
	Thermal conductivity	22 [W/m K]
	Heat capacity	500 [J/kg K]
	Rotational speed	41; 30; 23 [rad/s]

* Between the workpiece (wire) and the rigid parts of the model.

** Between all the rigid bodies of the model.

2.2. Material model

In a previous paper by the authors, the commercial software package DEFORM 3D™ was employed to model the material flow pattern inside the HYB PinPoint extruder, using the default flow stress data provided by the software material library Leoni et al. (2020a). To upgrade the material properties used as inputs to the simulations, the tensile test data reported by Leoni et al. (2020b) for the 1.4 mm diameter AA6082 wire are invoked and employed as a basis for a more comprehensive modelling. The aim is to model the FM flow stress as a function of accumulated strain ε, strain rate $\dot{\varepsilon}$ and temperature T, so that the output data cover all relevant ranges being applicable to the HYB process.

In the past different modelling approaches have been adopted. These include both physically-based, semi-empirical and fully empirical models Myhr et al. (2018), Gouttebroze et al. (2008), Jaspers (1999), Sekar et al. (2009). In the present paper a modified version of the Johnson-Cook constitutive equation is used as a starting point for the model development, which in its most general form reads Sekar et al. (2009):

$$\sigma(\varepsilon, \dot{\varepsilon}, T) = (A + B \cdot \varepsilon^n) \cdot \left(1 + C \cdot ln\left(\frac{\dot{\varepsilon}}{\dot{\varepsilon}_{ref}}\right)\right) \cdot \left(1 - E \cdot \left(\frac{T - T_{ref}}{T_{sol} - T_{ref}}\right)^m\right) \quad (1)$$

where A is the yield stress, B is the stress coefficient of the strain hardening, n is the power coefficient of the strain hardening, C is the strain rate coefficient, E is the thermal softening coefficient, m is the power coefficient of the thermal softening, $\dot{\varepsilon}_0$ is the reference value of the strain rate, T_{ref} is the chosen reference temperature (taken equal to room temperature RT) and T_{sol} is the solidus temperature of the FM.

In the Johnson-Cook equation the following six constants need to be determined from experiments, i.e. A, B, n, C, E and m by considering each of its three terms separately. Since all tensile tests carried out by Leoni et al. (2020b) were conducted at a constant strain rate $0.001\ s^{-1}$, the strain rate dependence of the flow stress (i.e. the constant C) was taken from Jaspers (1999), who performed experiments on AA6082 at various strain rates. The next step is to consider the specific case where $\dot{\varepsilon} = \dot{\varepsilon}_0$ and $T = T_{ref}$. In that case Equation (1) reduces to:

$$\sigma(\varepsilon) = (A + B \cdot \varepsilon^n) \quad (2)$$

where A is the true yield stress of the FM at RT (i.e. 25°C) and $\dot{\varepsilon}_0$=0.0001 s^{-1}. Based on Equation (2), the constants B and n can be determined by fitting the relationship to the true stress - true strain data reported for the FM at RT by Leoni et al. (2020b), which apply before the onset of necking.

Similarly, the calibration of the thermal softening coefficients can be done by first plotting the reported ultimate tensile strength data for the FM as a function of temperature, as illustrated in Figure 4, and then fitting Equation (1) to the experimental data points through adjustments of the parameters E and m.

The values of the constants A, B, n, C, E, m and T_{sol} used in the Johnson-Cook equation are listed in Table 2.

Table 2: Material constants used in the Johnson-Cook constitutive equation.

Material	A [MPa]	B [MPa]	n [/]	C [/]	E [/]	m [/]	T_{sol}[°C]
AA6082-T4	273	108	0.24	0.00747	1.14	0.762	582

It follows from the plots in Figure 5 that the Johnson-Cook constitutive equation is sufficiently relevant and comprehensive to allow the FM flow stress to be calculated as a function of temperature, accumulated strain and instantaneous strain rate. These data cover all relevant ranges being applicable to the HYB process Leoni et al. (2020a).

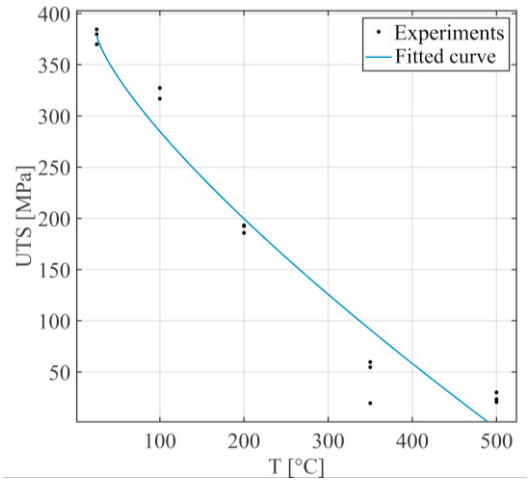

Figure 4: Fitting of Equation (1) to the UTS data reported by Leoni et al. (2020b) for the FM at different temperatures.

3. Results and discussion

Figure 6 shows snapshots of the situation during start-up of the filler wire feeding for the chosen combinations of wire diameters and drive spindle rotational speeds. These maps provide quantitative information about the material velocity fields and the equivalent stress fields within the FM. The values of the state variables are reflections of how effective the filler wire feeding is and how each wire responds to the imposed plastic deformation.

When the pin and the spindle tip (both being attached to the drive spindle) are rotating at a constant speed N_s, the inner extrusion chamber with its three moving walls will start to drag the filler wire both into and through the extruder due to the imposed friction grip. At the same time, it is kept in place inside the chamber by the stationary housing constituting the fourth wall. The response of the filler wires to the frictional forces acting on them during start-up can be deduced from the velocity field and stress field maps presented in Figure 6. A closer inspection reveals that these maps adequately capture the dependence of the filler wire feed rate on the spindle rotation speed. Moreover, Figure 6 shows that the stress level within the wires start to rise as soon as they enter the inlet hole in the housing. However, because the resulting wire distortions associated with these stress fields are small, there is no imminent risk of wire feeding problems neither for the ϕ1.2, the ϕ1.4 nor the ϕ1.6 mm filler wire during start-up.

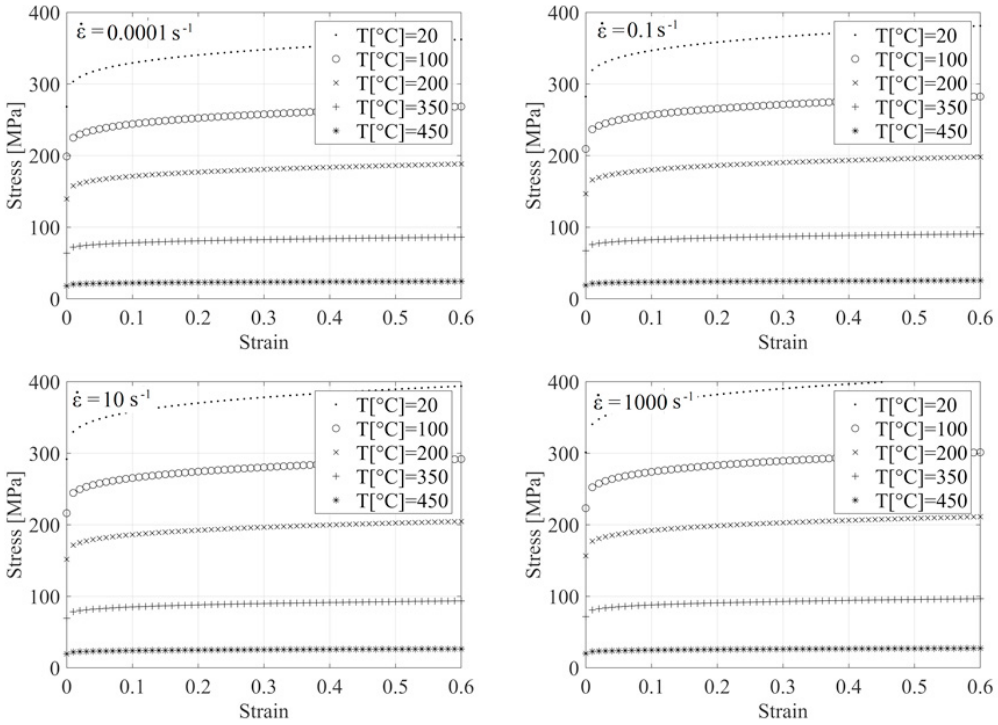

Figure 5: Graphical representations of predicted flow stress curves for the AA6082 FM.

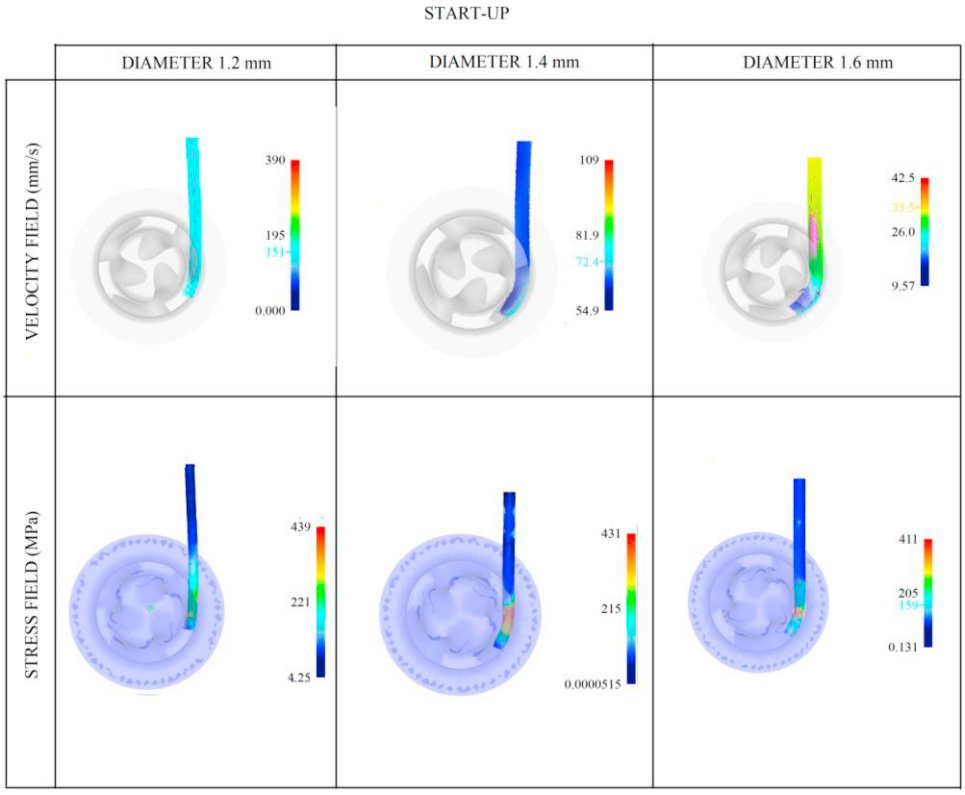

Figure 6: Calculated velocity field and stress field maps for the different filler wires during start-up of the wire feeding process.

After the tip of the filler wires has passed through the grip zone inside the housing, the aluminum is forced to flow against the abutment intersecting the extrusion chamber. When the required extrusion pressure in front of the abutment is reached, the FM starts to flow downwards in the axial direction and through the moving dies in the pin head. At this stage buckling of the wire inside the inlet hole in the extruder housing can be a problem, particularly if the stress level is high. In case the wire feeding becomes obstructed or completely blocked, the filler wire may physically break inside the extrusion chamber. This is because the strong pull forces acting on the enclosed wire will drag its front-end towards the abutment at the same time as its buckled tail-part resists the motion. As shown by the simulation results in Figure 7, the ϕ1.2 mm wire seems to be most vulnerable to buckling & breaking, but also the ϕ1.6 mm wire is inclined to this type of failure. Apparently, the ϕ1.4 mm wire is the best choice when it comes to minimizing the risk of wire feeding problems during extrusion & joining. This wire size is also the one that currently is used in the HYB process.

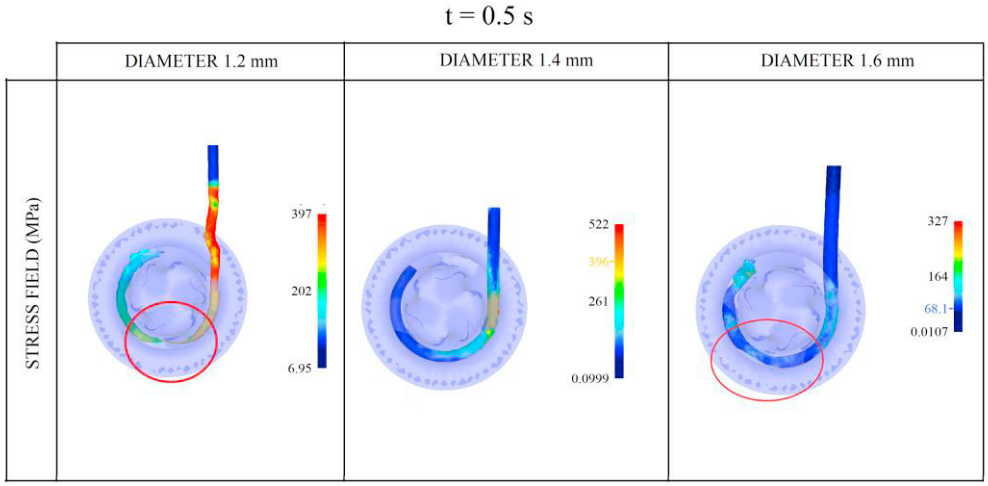

Figure 7: Calculated stress field maps for the different filler wires after they have reached the abutment and started to upset. The critical positions where either elongation or full separation of the elements occurs inside the extrusion chamber are indicated by the red circles in the maps.

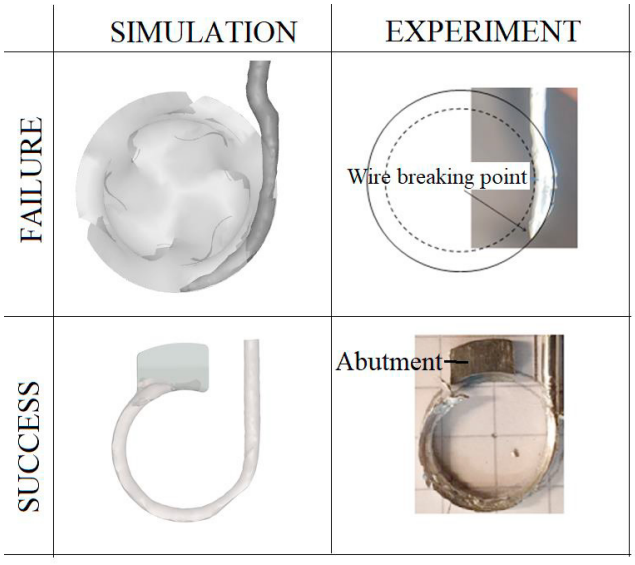

Figure 8: Examples of how the FE model can be used for daily problem solving and future process optimization.

Note the phenomenon of wire buckling & breaking is also something that is observed in a real joining situation, as shown by the photographs in Figure 8. In the HYB case it is the small "details" that make the difference between failure and success. The wire feeding problem is a good example of this, since even a minor misalignment of the extrusion chamber hight or width from start can cause a full stop in the wire feeding later during operation. Because the FE model is seen to capture the essence of the problem surprisingly well, it is deemed to be a powerful tool for both daily problem solving and further optimization of the HYB process.

4. Conclusions

In the HYB case, the filler wire feeding is a crucial part of the joining operation. Stable wire feeding is important to obtain adequate groove filling in a real welding situation.

Finite element (FE) modelling can be used to simulate the filler wire feeding in the HYB process. By importing CAD files of the PinPoint extruder into the commercial software package DEFORM 3D^{TM} simulations can run be under realistic conditions.

The Johnson-Cook constitutive equation can be used to model the filler metal flow stress as a function of accumulated strain, strain rate and temperature, based on experimental data acquired from tensile testing of the AA6082 filler wire. By importing data from the material model into the DEFORM 3D^{TM} software, quantitative information about the feeding behaviour of filler wires with diameters of 1.2, 1.4 and 1.6 mm, respectively has been obtained.

The simulations show that the ϕ1.4 mm wire is the best choice when it comes to minimizing the risk of buckling of the filler wire in the inlet hole of the housing, which subsequently can cause wire breaking inside the extrusion chamber. The use of smaller wire diameters (e.g. 1.2 mm) tends to enhance this wire feeding problem, but also the ϕ1.6 mm wire is seen to be inclined to buckling & breaking.

In the HYB case it is the small "details" that make the difference between failure and success. The wire feeding problem is a good example of this, since even a minor misalignment of the extrusion chamber hight or width from start can cause a full stop in the wire feeding later during operation. Because the FE model is seen to capture the essence of the problem surprisingly well, it is deemed to be a powerful tool for both daily problem solving and further optimization of the HYB process.

Acknowledgments

The authors acknowledge the financial support from HyBond AS, NTNU and NAPIC (NTNU Aluminium Product Innovation Center). They are also indebted to Tor Austigard and Ulf Roar Aakenes of HyBond AS for their help in providing the experimental data being used in the present study.

References

AWS Welding Handbook, 9th Ed., Volume 3, Welding Processes, Part 2, 2007. American Welding, Society, Miami, Florida (USA).

ASM Metals Handbook, Volume 6, Welding, Brazing and Soldering, 1993.ASM International, Materials Park, Ohio (USA).

F. Berto, L. Sandnes, F. Abbatinali, Ø. Grong and P. Ferro, 2018. "Using the Hybrid Metal Extrusion & Bonding (HYB) Process for Dissimilar Joining of AA6082-T6 and S355", Procedia Structural Integrity, Vol. 13, 249-254.

F. Leoni, Ø. Grong, L. Sandnes, T. Welo, F. Berto, 2020a. "Finite element modelling of the filler wire feeding in the hybrid metal extrusion & bonding (HYB) process", Journal of Advanced Joining Processes, Volume 1. DOI: https://doi.org/10.1016/j.jajp.2020.100006.

F. Leoni, Ø. Grong, L. Sandnes, F. Berto, 2020b. "High temperature tensile properties of AA6082 filler wire used for solid-state joining", Procedia Structural Integrity.

J. Blindheim, Ø. Grong, U. R. Aakenes, T. Welo and M. Steinert, (2018). "Hybrid Metal Extrusion & Bonding (HYB) - A New Technology for Solid-State Additive Manufacturing of Aluminium Components", Procedia Manuf., Vol. 26, 782–78.

K. Ulrich and S. Eppinger, 2008. "Product Design and Development - 4th Intern. Ed.", New York, USA, McGraw-Hill/Irwin.

L. Sandnes, Ø. Grong, J. Torgersen, T. Welo and F. Berto, 2018. "Exploring the Hybrid Metal Extrusion and Bonding Process for Butt Welding of Al–Mg–Si Alloys", Int. J. Adv. Manuf. Technol., Vol. 98, 1059-1065.

L. Sandnes, L. Romere, Ø. Grong, F. Berto and T. Welo, 2019. "Assessment of the Mechanical Integrity of a 2 mm AA6060-T6 Butt Weld Produced Using the Hybrid Metal Extrusion & Bonding (HYB) Process – Part II: Tensile Test Results", Procedia Structural Integrity, 17, 632–642.

M. Mazar Atabaki, M. Nikodinovski, P. Chenier, J. Ma, M. Harooni and R. Kovacevic, 2014. "Welding of Aluinium Alloys to Steels: An Overview", J. Manuf. Sci. Prod., 14 (2), 59-78.

O. R. Myhr, O. S. Hopperstad and T. Bjørvik, "A Combined Precipitation, Yield Stress, and Work Hardening Model for Al-Mg-Si Alloys

Incorporating the Effects of Strain Rate and Temperature", Metall. Mater. Trans. A, 49A, 3592-3609, 2018.
S. Gouttebroze, A. Mo, Ø. Grong, K. O. Pedersen and H. G. Fjær, "A New Constitutive Model for the Finite Element Simulation of Local Hot Forming of Aluminium 6xxx Alloys", Metall. Mater. Trans. A, 39A, 522-534, 2008.
S. Jaspers, 1999. "Metal Cutting Mechanics and Material Behavior", Eindhoven: Technische Universiteit Eindhoven.
S. Støren, "Analysis of the Conform Process Based on Experiences of Test Runs at HYDALU 17-20 August 1976", SINTEF Technical Note, Project No. 160182, No. 3, Trondheim, Norway, 1976.
V. Sekar, P. Kumar M, 2009. "Finite Element Analysis of the Effect of Cutting Speed on the Orthogonal Machining Process of AA6082(T6) Alloy" International Journal of Applied Engineering Research.
Ø. Grong, 2012. "Recent Advances in Solid-State Joining of Aluminium", Weld. J., 91, 26-33.
Ø. Grong, 1997. "Metallurgical Modelling of Welding", London, UK, Institute of Materials.
Ø. Grong, L. Sandnes and F. Berto, 2019. "A Status Report on the Hybrid Metal Extrusion & Bonding (HYB) Process and Its Applications", Mat. Design Process. Comm., 1, e41. https://doi.org/10.1002/mdp2.41.
Ø. Grong, L. Sandnes, T. Bergh, P.E. Vullum, R. Holmestad and F. Berto, 2019. "An Analytical Framework for Modelling Intermetallic Compound (IMC) Formation and Optimizing Bond Strength in Aluminium-Steel Welds, Mat. Design Process. Comm., 1, e57. https://doi.org/10.1002/mdp2.57, 2019.
Ø. Grong, L. Sandnes and F. Berto, 2019. "Progress in Solid-State Joining of Metals and Alloys", Procedia Structural Integrity, 17, 788–798.